Nanoscale

Accepted Manuscript

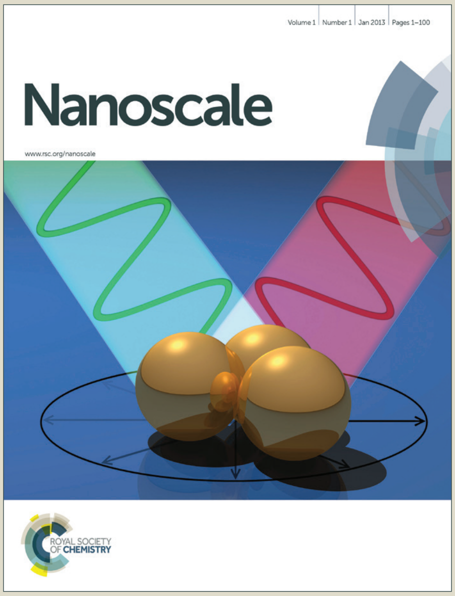

This is an *Accepted Manuscript*, which has been through the Royal Society of Chemistry peer review process and has been accepted for publication.

Accepted Manuscripts are published online shortly after acceptance, before technical editing, formatting and proof reading. Using this free service, authors can make their results available to the community, in citable form, before we publish the edited article. We will replace this *Accepted Manuscript* with the edited and formatted *Advance Article* as soon as it is available.

You can find more information about *Accepted Manuscripts* in the Information for Authors.

Please note that technical editing may introduce minor changes to the text and/or graphics, which may alter content. The journal's standard Terms & Conditions and the Ethical guidelines still apply. In no event shall the Royal Society of Chemistry be held responsible for any errors or omissions in this *Accepted Manuscript* or any consequences arising from the use of any information it contains.

ROYAL SOCIETY OF CHEMISTRY

www.rsc.org/nanoscale

Nanoscale RSCPublishing

COMMUNICATION

Cite this: DOI: 10.1039/x0xx00000x

Received 00th January 2014,
Accepted 00th January 2014

DOI: 10.1039/x0xx00000x

www.rsc.org/nanoscale

The selective formation of graphene ranging from two-dimensional sheets to three-dimensional mesoporous nanospheres

Jian Wang,[a] HuileJin,[a] Yuhua He,[a] Dajie Lin,[a] Aili Liu,[a] Shun Wang,*[a] and Jichang Wang*[a, b]

This research presents a template-free solvothermal method which offers the selective preparation of graphene ranging from two-dimensional sheets to 3-dimensional nanospheres. The thus prepared nanospheres have size-defined mesopores with a huge surface area and, after doping with nitrogen, exhibited stronger electrocatalytic activity toward oxygen reduction than commercial Pt/C catalysts.

Graphene has recently been intensively exploited for wide applications in medicine, biology, catalysis, environmental protection, energy storage and conversion, to name a few.[1] To utilize the combining advantages from both graphene and porous materials in a 3-dimensional (3D) configuration, there are increasing efforts to fabricate 3D porous graphene materials (PGM) due to their large surface areas, unique porous structures, diversified compositions and excellent electronic conductivity.[2-4] Macroporous graphenes formed through self-assemblies,[2] graphene bubble networks derived from templated chemical vapour deposition or sugar-blowing approach [3] and porous graphene hybrids by physical/chemical assemblies on functional metals, oxides, polymers or carbon nanotubes (CNT) connectors [4] have been reported in the last several years. However, several key points remain to be addressed in the synthesis and application of 3D PGM. First, the synthesis of 3D PGM has so far relied on templates, in which either a soft or a hard template is deployed to provide the needed 3D microstructure.[2] The removal of template does not only complicate the fabrication procedure, but also increases the final cost. Second, the reported 3D PGM almost based on RGO and its derivates,[2,4] the restored electrical conductivity of RGO is inferior to pristine graphene. Although 3D PGM from CVD technique exhibit impressive conductivity, their processability and fabrication cost are the critical issue hampering massive commercial application.[3]Third, few approaches can be directly applied to control over the pore morphology, including size and wall thickness, in the construction of 3D PGM. To address these issues, we report a bottom-up template-free solvothermal method for selective formation of graphene from two-dimensional sheets to 3D nanospheres. The selection was accomplished by simply tuning the reaction pressure. These as-prepared novel 3D mesoporous graphene (MG) have a huge accessible surface area and size-defined mesopores for electron/electrolyte transportation. These features enable the 3D MG nanopheres to serve as a key candidate for diverse practical usages, for example, high-performance non-metal electrocatalyst for oxygen reduction reaction (ORR), as highlighted in this research.

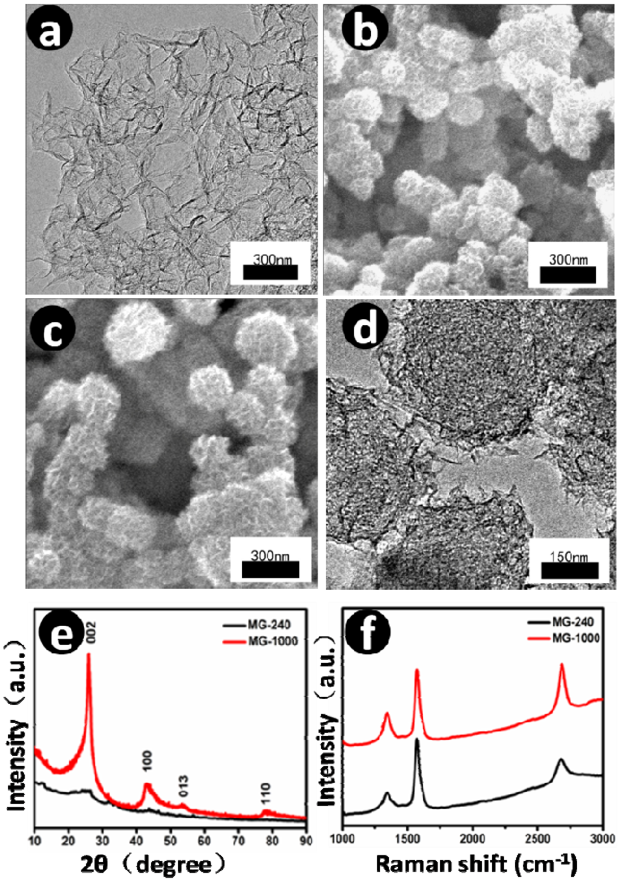

Figure 1.(a) TEM, (b) SEM, and (c) SEM images of graphene prepared under different reaction conditions; (d) TEM, (e) XRD, and (f) Raman spectra of the graphene nanospheres shown in (c).

Nanoscale Accepted Manuscript

Our template-free solvothermal synthesis involves the reduction of hexachlorobutadiene by sodium in an autoclave at a moderate temperature, in which the reaction pressure was employed as a means to manipulate the morphology of the final products. Figure 1a presents a transmission electron microscopy (TEM) image of graphene formed at a condition that the autoclave was only partially filled with the reactant hexachlorobutadiene. This image demonstrates that graphene sheets are the dominant reaction product. If the empty portion of the autoclave was filled with 5.0 MPa argon gas, while all other conditions were kept the same as those used in Figure 1a, the graphene products turned into nanospheres with a very rough surface (see Figure 1b). To further examine the importance of reaction pressure in the development of the above 3D morphology, solvothermal reactions were also conducted at a configuration where the autoclave was completely filled with hexachlorobutadiene, where thermal expansion of hexachlorobutadiene liquid in response to the elevated temperature caused pressure increase. As shown in Figure 1c, porous graphene nanospheres were also obtained under such conditions.

TEM (Figure 1d) and HRTEM (Figure S1 in the supporting information) indicate that those nanospheres are made up by single and few-layer graphene sheets. This suggestion is supported by the following XRD and Raman spectra. Crumpling of graphene sheet to form 3D materials has been reported by Huang and coworkers when graphene solution was dried rapidly.[5] The products analyzed above were collected through centrifugation at 8000 rpm and were dried at 240 ℃ for 2 h under the protection of argon. The drying process ensures that no hexachlorobutadiene residue was left inside the 3D PGM, since the boiling temperature of hexachlorobutadiene is about 230 ℃. Thermogravimetric analysis (TGA) also confirms that drying at 240 ℃ removes hexachlorobutadiene residues (see Figure S2 in the supporting information). The dried graphene nanospheres is denoted as MG-240. For thermal treatment, MG-240 was heated to different preselected temperature such as 800,900,1000,1100, or 1200 ℃ for 1 h under the protection of argon. The thus-obtained graphene products are denoted as MG-800, MG-900, MG-1000, MG-1100 and MG-1200 in the following discussion.

XRD spectra in Figure 1e indicate that heat-treatment caused an increase in the crystallity of the 3D PGM, where the highest peak (002) is consistent with the fringe space seen in the HRTEM image (Figure S1 in the supporting information). Figure 1f presents the Raman spectra of MG-240 and MG-1000. The presence of a 2D-band at 2720 cm^{-1} suggests that the graphene products consist of mainly few-layer sheets.[6] After heat-treatment, the D band at 1365 cm^{-1} is enhanced, implicating the presence of increasing number of edges and defects. This structural change might be responsible for the increase of gas adsorption seen in this study. The above XRD and Raman measurements suggest that the as-prepared nanospheres are made up of graphene sheets. Notably, the morphology of these nanospheres remains intact after heat treatment and nitrogen-doping, highlighting the strong mechanical property of the 3D PGM (see Figures S2a and S2b in supporting information).

Figure 2a presents the nitrogen gas adsorption-desorption isotherms of MG-240, MG-1000 and NMG-1/4. Here, NMG-1/4 denotes the nitrogen-doped MG-240 that doping was conducted at a1:4 molar ratio of MG-240 and urea. The results show that uponheat-treatment at 1000 ℃ for 1 hour, the nitrogen adsorption of graphene spheres is significantly increased. Steps in the isotherms indicate the porous structure of the materials. Influences of thermal treatment as well as nitrogen-doping on the specific surface area and pore size distribution of the graphene nanospheres are explored in this study (see Table 1 in the supporting information).According to the data, the increase in gas adsorption of MG-1000 shall be attributed to the dramatic increase in its specific surface area. After doping with nitrogen, the gas adsorption increases further. However, nitrogen-doping does not improve the specific surface area, where the surface area and the pore volume are actually decreased slightly. The improvement in gas adsorption therefore must arise from other factors, for instance, changes in the surface electronegativity caused by nitrogen insertion. Pore size distribution presented in Figure 2b indicates that the pore structure of MG-1000 and NMG-1/4 nanospheres is sharply centered at 4 nm (i.e., showing mesoporous feature).

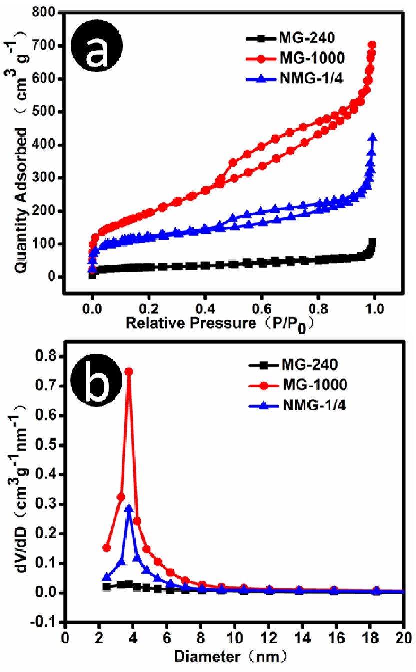

Figure 2. (a) Nitrogen adsorption/desorption curves, and (b) pore size distribution ofMG-240, MG-1000 and NMG-1/4 products.

The forms and level of doped nitrogen atom (i.e., graphitic, pyrrolic or pyridinic) have been characterized with XPS. Those measurements (Figure S3a in the supporting information) illustrate that for the graphene products without heat-treatment there is a tiny chorine peak in the XPS spectrum. After heat-treatment at 1000 ℃ for 1 hour, the chlorine peak disappears and only C 1s peak is observable. The chlorine peak is thereforelikely arising from hexachlorobutadiene residue, rather than from theformation of chlorine-doped graphene. Upon reacting with urea at 1000 ℃, an N1s peak emerges in the XPS spectrum. Such a peak grew stronger as the amount of urea in the initial mixture was increased. From XPS spectra the nitrogen content in the doped graphene nanospheres was estimated to have increased from 0.6 to 1.5 percent as the graphene/urea ratio was adjusted from 1:1 to 1:4. Increasing the urea/graphene molar ratio above 4 did not lead to further improvement of the nitrogen content. These nitrogen atoms exist in three different forms (see Figures S3b to S3d in the supporting information). Literature has suggested that pyrrolic form nitrogen was responsible for the high electrocatalytic activity of nitrogen-doped carbon materials in the ORR in alkaline solution.[7]

Electrocatalyticactivity of the above as-prepared and nitrogen-doped graphene sheets and nanospheres toward ORR was examined through cyclic voltammetry (CV) and linear sweep voltammetry (LSV) at a rotating disk electrode (RDE) in alkaline solution. The undoped graphene is not as effective as those doped materials.

Nanoscale Accepted Manuscript

This journal is © The Royal Society of Chemistry 2014

Shown in Figures 3a and 3b are the results obtained with NMG-1/4. In the absence of O_2, the behavior of the working electrode looks like a normal double-layer capacitor with a rapid charge/discharge current change. Same as earlier report of mesoporous carbon materials,[8] a notable anodic peak is seen in the O_2-saturated KOH solution, which is attributed to the reduction of oxygen molecules. The onset potential of O_2 reduction is about -0.1 V vs AgCl/Ag reference electrode. This is a favorable result in comparison to what has been obtained with commercial Pt/C electrode and other nitrogen-doped carbon materials.[9] Figure 3b shows that the current density increases as the disk rotation speed is increased from 400 to 3600 rpm. The transferred electron number per O_2 molecule involved in this ORR process was determined by Koutecky-Levich equation, which relates the current density j to the rotation rate of the electrode. In Figure 3c the corresponding Koutecky-Levich plots at various electrode potentials exhibit a good linearity, indicating the first-order reaction kinetics with respect to the concentration of dissolved O_2. The *n* value for the NMG-1/4 is derived to be 3.6 – 3.9 at the potential ranging from -0.3 to -0.4 V, suggesting a four-electron process for the ORR.

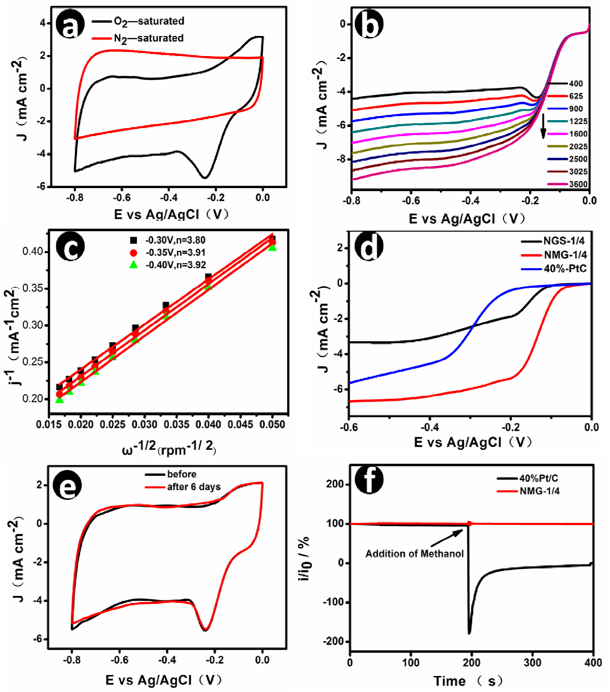

Figure 3. (a) Cyclic voltammetry of nitrogen and oxygen saturated alkaline solution, (b) linear sweep voltammetry of oxygen saturated solution under different rotating rate of the disc electrode, (c) Koutecky-Levich plot (J^{-1} versus $\omega^{-1/2}$) at different electrode potentials, (d) Linear sweep voltammetry of NMG-1/4，NGS-1/4 and commercial Pt/C, (e) cyclic voltammogram at different reaction times, and (f) chronoamperometric response of NMG-1/4 electrode and commercial Pt-C electrode to methanol addition. Electrodes used in (a), (b), (c) and (e) are made of NMG-1/4.

LSV in Figure 3d indicates that the current density obtained with NMG-1/4 is stronger than that of the commercial 40% Pt/C catalyst, while the onset potential of the ORR is also more positive at the nitrogen-doped graphene electrode. The disk rotation rate in Figure 3d is 1600 rpm. The NGS-1/4 denotes nitrogen-doped graphene sheets that were shown in Figure 1a. The doping procedure for graphene sheets is the same as that used for graphene nanospheres. LSV in Figure 3d illustrate that doped graphene mesoporous nanospheres outperformed graphene sheets in the ORR, highlighting the advantages of 3D MG nanospheres due to their large surface areas, unique porous structures, and excellent electronic conductivity.

To evaluate the stability of the as-obtained 3D MG nanospheres, in particular nitrogen-doped graphene NMG-1/4 electrode, CVs of an O_2-saturated 0.1 M KOH solution was run continuously for several days. Shown in Figure 3e are CVs collected at the start of the measurement (light colored curve) and after 6 days (dark curve). The two CVs almost overlap with each other, suggesting that nitrogen-doped nanospheres prepared in this research are stable and can endure the long term operation of ORR. This is a great improvement in comparison to what was seen with the Pt-C/GC electrode which exhibited a fast current decrease. To examine the alcohol poisoning of the nitrogen-doped graphene nanospheres (i.e., cross-over effect) versus the commercial Pt-C electrode, current-time (*i*–*t*) chronoamperometric responses of both electrodes to the addition of 2% (v/v) methanol was investigated. The results in Figure 3f demonstrate that the nitrogen-doped graphene electrode does not produce any change in the current, whereas a great and rapid change at the commercial Pt-C electrode is seen (i.e., being rapidly poisoned by methanol).

In summary, we have demonstrated that graphene can be selectively fabricated from 2D sheets to 3D nanospheres by conveniently adjusting the reaction pressure of this solvothermal synthesis. As illustrated by the results obtained at moderate gas phase pressures (see Figure S9) the portion of graphene spheres in the final products increases with the reaction pressure. Notably, this bottom-up synthetic procedure is robust, allowing us to obtain 3D flowerlike PGM with size-defined mesopores and consistent electrochemical properties (i.e., LSV and ORR performance). The produced MG nanospheres appear to be spatially assembled by single and few-layer graphene sheets, which effectively prevent graphene from taking face to face aggregation. The above observed morphological change is most likely resulting from physical factors, say, hydrodynamics (i.e. the micro flow/convection of the reaction solution). It is well known that increasing gas phase pressure elevates the boiling temperature. As such, liquid is expected to undergo less turbulent/vigorous motion under higher gas pressure. The less vigorous micro motion of the reaction solution subsequently allows the 2D graphene sheets to fold and aggregate to evolve into a 3D microstructure.

The 3D topological configuration yields a large specific surface area and unique size-defined mesopores, while maintaining the excellent conductivity exhibited by graphene sheet. These unordinary features enable 3D MG nanospheres to serve as an attractive candidate for many graphene-related applications, such as sensing, gas storage, chemical separation, selective catalysis, nanocomposition, high-performance energy storage and conversion, to name a few. The results complement recent efforts of making hybrid graphene-based non-metal catalysts with 3D PGM in order to harvest the thermal/electrical properties of graphene along both in-plane as well as out-of-plan directions.[10] As a case study, the nitrogen-doped MG nanospheres did exhibit higher electrocatalytic activity, better stability, and superior tolerance to the methanol crossover effect toward ORR than that of commercial Pt/C catalysts.

We are grateful for financial supports from NSFC (21073133, 51272182 and 21301130), Zhejiang Provincial Natural Science Foundation of China (LY13E020008) and Zhejiang Scientific and technological innovation fund (2013R424067).

Notes and references

Nanoscale Accepted Manuscript

[a]Nano-materials and Chemistry Key Laboratory, WenzhouUniversity, Wenzhou, Zhejiang, China 325027. Email: Shunwang@wzu.edu.cn.
[b]Department of Chemistry and Biochemistry, University of Windsor, Windsor, ON, Canada N9B3P4. Email: jwang@uwindsor.ca.

† Electronic Supplementary Information (ESI) available. Detailed experimental procedures, HRTEM, TGA and Mass spectroscopy, Raman spectra, additional synthetic results at different reaction temperatures and results with graphene sheets. See DOI: 10.1039/c000000x.

1 (a)A. K. Geim, K .S. Novoselov,*Nat. Mater.*2007, **6**, 183; (b) A. K. Geim, *Science*, 2009, **324**, 1530; (c) K. S. Kim, Y. Zhao, H. Jang, S. Y. Lee, J. M. Kim, K. S. Kim, J. H. Ahn, P. Kim, J. Y. Choi, B. H. Hong, *Nature*, 2009, **457**, 706; (d) M. J. Allen, V. C. Tung, R. B. Kaner, *Chem. Rev.* 2010, **110**, 132; (e) F. Bonaccorso, Z. Sun, T. Hasan, A. C. Ferrari, *Nat. Photon.* 2010, **4**, 611; (f) D. Chen, L. Tang, J. Li, *Chem. Soc. Rev.*2010, **39**, 3157; (g) Y. Sun, Q. Wu, G. Shi, *Energy Environ. Sci.* 2011, **4**, 1113; (h) Y. U. Zhu, S. Murali, M. D. Stoller, K. J. Ganesh, W. W. Cai, P. J. Ferreira, A. Pirkle, R. M. Wallace, K. A. Cychosz, M. Thommes, D. Su, E. AStach, R. S. Ruoff, *Science*, 2011,**332**, 1537; (i) Y. Y. Liang, Y. G. Li, H. L. Wang, J. G. Zhou, J. Wang, T. Regier, H. J Dai, *Nat. Mater.* 2011, **10**, 780; (j) Z. Yang, Z. Yao, G. Li, G. Fang, H. Nie, Z. Liu, X. Zhou, X. A.Chen, S. Huang, *ACS Nano* 2011, **6**, 205; (k) Y. Li, Y. Zhao, H. H.Cheng, Y. Hu, G. Shi, L. Dai, L. Qu, *J. Am. Chem. Soc.* 2012, **134**, 15; (l) X. Huang, X. Y. Qi, F. Boey, H .Zhang, *Chem. Soc. Rev.*2012, **41**, 666; (m) L. Dai, *Acc. Chem. Res.* 2013, **46**, 31.

2 (a) S. Z. Zu, B. H. Han, *J. Phys. Chem. C,* 2009, **113**, 13651, (b) Y. Xu, K. Sheng, C. Li, G. Shi, *ACS Nano*, 2010, **4**, 4324; (c) S. H. Lee, H. W. Kim, J. O. Hwang, W. J. Lee, J. Jwon, C. W. Bielawski, R. S. Ruoff, S. O.Kim, *Angew. Chem. Int. Ed.* 2010, **49**, 10084. (d) S. Yin, Y. Zhang, J. Kong, C. Zou, C. M. Li, X. Lu, J. Ma, F. Y. C. Boey, X. Chen, *ACS Nano* 2011, **5**, 3831; (e) J. H. Liu, G. S. Chen, M. Jiang, *Macromolecules* 2011, **44**, 7682; (f) Z. S. Wu, A. Winter, L. Chen, Y. Sun, A. Turchanin, X. Feng, K. Müllen, *Adv. Mater.* 2012, **24**, 5130; (g) S. Srinivasan, W. H. Shin, J. W. Choi, A. Coskun, *J. Mater. Chem. A,* 2013, **1**, 43;(h) S. Han, D.Wu, S. Li, F. Zhang, X. Feng, *Adv. Mater.* 2013,**26**, 849.

3 (a) Z.Chen, W. Ren, L. Gao, B. Liu, S. Pei, H. M. Cheng, *Nat. Mater.* 2011, **10**, 424; (b) B. G. Choi, M. Yang, W. H. Hong, J. W. Choi, Y. S. Huh, *ACS Nano,* 2012, **6**, 4020;(c) Y. C. Yong, X. C. Dong, M. B. Chan-Park, H. Song, P. Chen, *ACS Nano* 2012, **6**, 2394;(d) X. Wang, Y. Zhang, C. Zhi, X. Wang, D. Tang, Y. Xu, Q. Weng, X. Jiang, M. Mitome, D. Golberg, Y. Bando, *Nat. Commun.* 2013, **4**, 2905; (e) M. Wang, L. Fu, L. Gan, C. Zhang, M. Ruemmeli, A. Bachmatiuk, K. Huang, Y. Fang, Z. Liu, *Sci. Rep.* 2013, **3**, 1238.

4 (a) J. L.Vickery, A. J. Patil, S. Mann, *Adv. Mater.*2009, **21**, 2180; (b) V. C. Tung, L.Chen, M. J. Allen, J. K.Wassei, K. Nelson, R. B. Kaner, Y.Yang, *ACS Nano*, 2009, **9**, 1949;(c) S. Guo, S. Dong, *Chem. Soc. Rev.* 2011, **40**, 2644; (d) Y. G. Li, W. Zhou, H. L. Wang, L. M. Xie, Y. Y. Liang, F. Wei, J. C. Idrobo, S. J. Pennycook, H. J. Dai, *Nat. Nanotechnol.* 2012, **7**, 394; (e) X. Huang, K. Qian, J. Yang, J. Zhang, L. Li, C. Yu, D. Zhao, *Adv. Mater.* 2012,**24**, 4419.

5 (a) J. Luo, H. D. Jang, T. Sun, L. Xiao, Z. He, A. P. Katsoulidis, M. G. Kanatzidis, J. M. Gibson, J. Huang,*ACS Nano,* 2011, **5**, 8943;(b) J. Luo, H. D. Jang, J. Huang, *ACS Nano,* 2013, **7**, 1464.

6 (a)F. Tuinstra, J. L Koenig, *J. Chem. Phys.,* 1970, **53**, 1126; (b) A. Ferrari, J. Meyer, V. Scardaci, C. Casiraghi, M. Lazzeri, F. Mauri, S. Piscanec, D. Jiang, K. Novoselov, S. Roth, *Phys. Rev. Lett.* 2006, **97**, 187401.

7 (a) L. Qu, Y. Liu, J. B. Baek, L. Dai, *ACS Nano,* 2010, **4**, 1321; (b) Y. Zhang, J. Ge, L. Wang, D. Wang, F. Ding, X. Tao, W. Chen, *Sci. Rep.* 2013, **3**,2771.

8 (a) D. S.Yang, D. Bhattacharjya, S.Inamdar, J. Park, J. S.Yu, *J. Am. Chem. Soc.,* 2012, **134**, 16127; (b) S. Chen, J. Bi, Y. Zhao, L. Yang, C. Zhang, Y. Ma, Q. Wu, X. Wang , Z. Hu. *Adv Mater.*2012, **24**, 5593;(c)T. P. Fellinger, F. Hasche, P. Strasser, M. Antonietti, *J. Am. Chem. Soc.,* 2012, **134**, 4072; (d) R. Silva, D. Voiry,M. Chhowalla , T. Asefa, *J. Am. Chem. Soc.,* 2013, **135**, 7823.

9 (a) K. Gong, F. Du, Z. Xia, M. Durstock, L. Dai, *Science,* 2009, **323**, 760; (b) S. Kundu, T. C. Nagaiah, W. Xia, Y. Wang, S. V. Dommele, J. H. Bitter, M. Santa, G. Grundmeier, M. Bron, W. *J.* Schuhmann, *Phys.Chem. C,* 2009, **113**, 14302;(c) L. Zhang, J. Niu, L. Dai, Z. Xia, *Langmuir,*2012, **28**, 7542.

10 (a) J. C. Meyer, A.Geim, M.Katsnelson, K. Novoselov, T. Booth, S. Roth, *Nature,*2007, **446**, 60; (b) Z. S. Wu, W. Ren, L. Gao, J. Zhao, Z. Chen, B. Liu, D. Tang, B. Yu, C. Jiang, H. M. Cheng, *Acs Nano,* 2009, **3**, 411.

Nanoscale Accepted Manuscript

This journal is © The Royal Society of Chemistry 2014